

# **ELECTRON THERMAL TRANSPORT IN ENHANCED CORE CONFINEMENT REGIMES**

by

**G.M. STAEBLER, R.E. WALTZ, C.M. GREENFIELD, B.W. STALLARD,  
M.E. AUSTIN, K.H. BURRELL, J.S. deGRASSIE, E.J. DOYLE,  
R.J. GROEBNER, G.L. JACKSON, M. KOTSCHENREUTHER, L.L. LAO,  
Y.R. LIN-LIU, T.C. LUCE, M. MURAKAMI, C.C. PETTY, R.I. PINSKER,  
P.A. POLITZER, R. PRATER, C.L. RETTIG, T.L. RHODES, B.W. RICE,  
R.D. STAMBAUGH, H.E. ST. JOHN, and W.P. WEST**

**JULY 1998**

## DISCLAIMER

This report was prepared as an account of work sponsored by an agency of the United States Government. Neither the United States Government nor any agency thereof, nor any of their employees, makes any warranty, express or implied, or assumes any legal liability or responsibility for the accuracy, completeness, or usefulness of any information, apparatus, product, or process disclosed, or represents that its use would not infringe privately owned rights. Reference herein to any specific commercial product, process, or service by trade name, trademark, manufacturer, or otherwise, does not necessarily constitute or imply its endorsement, recommendation, or favoring by the United States Government or any agency thereof. The views and opinions of authors expressed herein do not necessarily state or reflect those of the United States Government or any agency thereof.

# ELECTRON THERMAL TRANSPORT IN ENHANCED CORE CONFINEMENT REGIMES

by

G.M. STAEBLER, R.E. WALTZ, C.M. GREENFIELD, B.W. STALLARD,<sup>†</sup>  
M.E. AUSTIN,<sup>‡</sup> K.H. BURRELL, J.S. deGRASSIE, E.J. DOYLE,<sup>△</sup>  
R.J. GROEBNER, G.L. JACKSON, M. KOTSCHENREUTHER,<sup>‡</sup> L.L. LAO,  
Y.R. LIN-LIU, T.C. LUCE, M. MURAKAMI,<sup>◇</sup> C.C. PETTY, R.I. PINSKER,  
P.A. POLITZER, R. PRATER, C.L. RETTIG,<sup>△</sup> T.L. RHODES,<sup>△</sup> B.W. RICE,<sup>†</sup>  
R.D. STAMBAUGH, H.E. ST. JOHN, and W.P. WEST

This is a preprint of a paper to be presented at the 25th European Physical Society Conference on Controlled Fusion and Plasma Physics, June 29–July 3, 1998, Prague, Czech Republic, and to be published in the *Proceedings*.

<sup>†</sup>Lawrence Livermore National Laboratory

<sup>‡</sup>University of Texas, Austin

<sup>△</sup>University of California, Los Angeles

<sup>◇</sup>Oakridge National Laboratory

Work supported by  
the U.S. Department of Energy  
under Contracts DE-AC03-89ER51114, W-7405-ENG-48,  
DE-AC05-96OR22464, and Grant DE-FG03-86ER53266

GA PROJECT 3466  
JULY 1998

## ELECTRON THERMAL TRANSPORT IN ENHANCED CORE CONFINEMENT REGIMES\*

G.M. Staebler, R.E. Waltz, C.M. Greenfield, B.W. Stallard,<sup>†</sup> M.E. Austin,<sup>‡</sup> K.H. Burrell, J.S. deGrassie, E.J. Doyle,<sup>Δ</sup> R.J. Groebner, G.L. Jackson, M. Kotschenreuther,<sup>‡</sup> L.L. Lao, Y.R. Lin-Liu, T.C. Luce, M. Murakami,<sup>◇</sup> C.C. Petty, R.I. Pinsky, P.A. Politzer, R. Prater, C.L. Rettig,<sup>Δ</sup> T.L. Rhodes,<sup>Δ</sup> B.W. Rice,<sup>†</sup> R.D. Stambaugh, H.E. St. John and W.P. West

*General Atomics, P.O. Box 85608, San Diego, CA 92186-5608*

The cause of the anomalous electron thermal transport in a region of suppressed ion thermal transport is investigated using a comprehensive gyrokinetic stability code [1]. Analysis of a DIII-D negative central shear discharge with additional fastwave electron heating is presented. It is found that the electron heating excites the electron temperature gradient mode (ETG). The enhanced electron thermal transport from power balance analysis is consistent with the increased growth rate for the ETG mode. The ion thermal transport barrier is observed to retreat towards the plasma center during the fastwave heating (FW). Transport modeling with self-consistent  $E \times B$  velocity shear reproduces this effect for on-axis electron heating. The same transport model predicts that off-axis electron heating can extend the region of reduced transport outward.

The suppression of turbulence by  $E \times B$  velocity shear has been shown to explain the formation of regions of neoclassical ion thermal transport reduction quite well [2]. These internal transport barrier (ITB) regions also offer the opportunity to study the subdominant turbulent transport mechanisms in tokamaks. Since only the ions reach the neoclassical minimum level of thermal transport, there remains an anomalous electron heat loss. The new challenge is to understand the origin of the electron anomaly. Gyrokinetic stability calculations of linear growth rates show that the  $E \times B$  velocity shear within the ITB is larger than the linear growth rates (without  $E \times B$  velocity shear) for the ion temperature gradient mode (ITG) and trapped electron mode (TEM). Non-linear simulation of ITG turbulence predicts complete quenching of turbulence under this condition [3]. However, the ETG mode is calculated to be unstable within the ITB with a growth rate much higher than the  $E \times B$  velocity shear. Thus, the ETG mode can survive within the ITB. The ETG mode has a high wavenumber compared to the ITG mode and is predicted from quasilinear theory to mostly cause electron thermal transport. The electron thermal transport can be probed by heating electrons. The addition of electron heating within the ITB, with either fastwave or electron cyclotron heating on-axis, has been found to cause the ITB to shrink towards the center. This is illustrated in Fig. 1 for DIII-D discharge 89986. This was an upper single-null plasma ( $B_T=2.1$  T,  $\kappa_{sep}=1.94$ ,  $\delta_{sep}^{top}=0.9$ ,  $\delta_{sep}^{bot}=0.4$ ,  $R_{axis}=1.8$  m,  $a=0.6$  m). The ITB was established by the addition of 5 MW of co-injected neutral beam power during the current ramp phase [Fig. 1(a)]. This results in a safety factor profile with a negative shear ( $q$  on axis =3.6,  $q_{min}=2.7$  at  $\rho=0.62$ ,  $q_{95}=5.7$  at 1.05s). The core ion temperature continues to rise as the

---

\*Work supported by U.S. Department of Energy under Contracts DE-AC03-89ER51114, W-7405-ENG-48, DE-AC05-96OR22464, and Grant No. DE-FG03-86ER53266.

<sup>†</sup>Lawrence Livermore National Laboratory.

<sup>‡</sup>University of Texas, Austin.

<sup>Δ</sup>University of California, Los Angeles.

<sup>◇</sup>Oak Ridge National Laboratory.

leading edge of the ITB grows outward until the fastwave heating begins at 1.1s [Fig. 1(b)]. The central fastwave electron heating causes a prompt rise in the core electron temperature [Fig. 1(c)], but the core ion temperature drops. The radial profiles of the ion and electron temperatures at the times marked by dashed vertical lines in Fig. 1 just before (1.0s) and during (1.2s) the fastwave heating are shown in Fig. 2. The steep gradient region of the ion temperature is seen to retreat towards the axis in Fig. 2(b). A similar change occurs in the carbon toroidal rotation Fig. 2(d), but the electron density continues its steady rise begun at the start of the neutral beams Fig. 2(c). The ITB expands again after the increase in neutral beam power at 1.35 s. Since the ITG growth rate is known to be reduced by hot ions  $T_i/T_e > 1$ , it would be expected that electron heating could destabilize the ITG modes and explain the shrinking ITB. This expectation is not born out by the linear stability calculations which show a reduction in the ITG growth rate due to the reduction in the ion temperature gradient. The gyrokinetic growth rate spectrum is displayed in Fig. 3 for the two times (1.0 s before FW, 1.2 s during FW) at several locations. It is useful to plot the ratio of the growth rate  $\gamma$  to the poloidal wavenumber  $k_\theta$  verse the poloidal wavenumber on a logarithmic scale. The area under the curve is then proportional to the mixing length estimate for the turbulent diffusivity  $\chi \propto \int d\log(k_\theta) \rho_i \gamma/k_\theta$ . Also included in Fig. 3. is the local  $E \times B$  shear rate  $\Omega_{E \times B}$  computed from the carbon charge exchange measurement. According to the  $E \times B$  shear quench rule [3] all growth rates (computed without  $E \times B$  shear) which fall below the  $E \times B$  shearing rate are suppressed and do not contribute to transport. The growth rates are computed with a linear stability code [1] including the fully

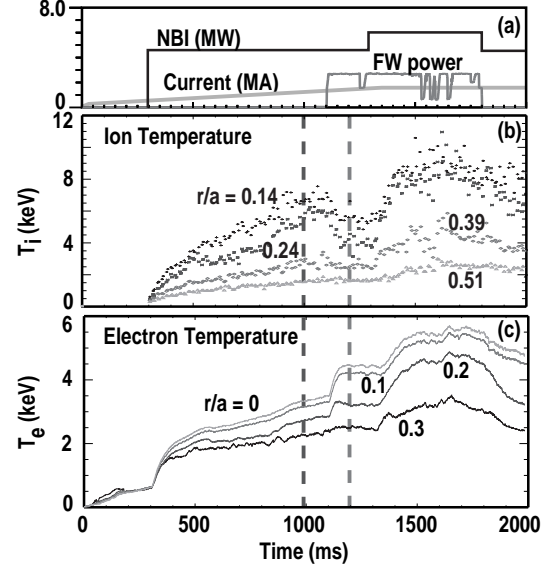


Fig. 1. Overview of DIII-D discharge 89986 showing (a) neutral beam heating power, fast wave heating power and toroidal plasma current (b), ion temperature and (c) electron temperature.

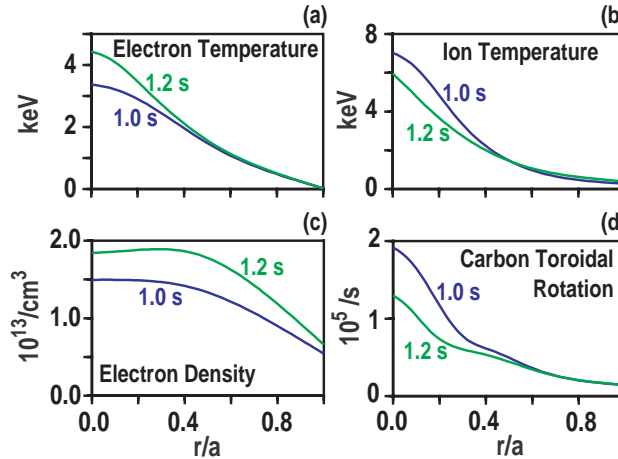


Fig. 2. Radial profiles of (a) electron temperature, (b) ion temperature, (c) electron density and (d) carbon toroidal rotation frequency both before (1.0s) and during (1.2s) fast wave heating.

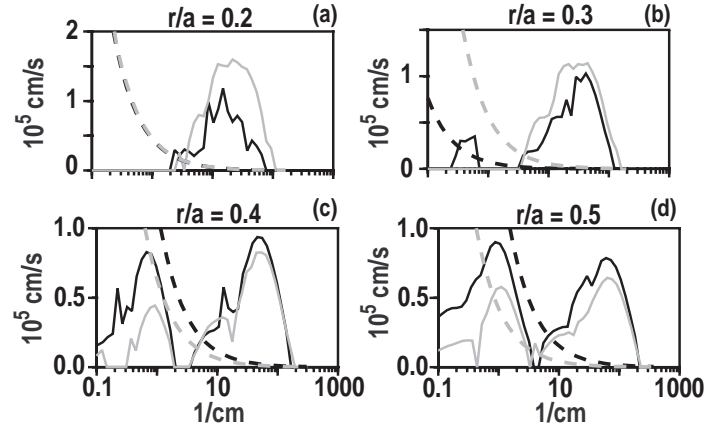


Fig. 3. Spectrum of drift wave growth rates/wave number (solid curves) versus wave number (logarithmic scale) at 1.0 s (black) and 1.2 s (grey) and for locations  $r/a=0.2, 0.3, 0.4, 0.5$ . Also shown are the measured  $E \times B$  velocity shear/wave number (dashed curves) for the same times and locations.

kinetic response for the electrons and two ion species (deuterium and carbon). The code is limited to high toroidal wavenumber ballooning modes in a shifted circle model magnetic geometry. The electrostatic limit has been used for the present calculations which is a good approximation for pressures below the ideal magnetohydrodynamic ballooning mode limit. Near the axis [ $r/a=0.2$ , Fig. 3(a)] the high wavenumber ETG modes are excited by the electron heating. Even though  $T_i/T_e$  decreased, the low  $k$  part of the spectrum (ITG, TEM) remains linearly stable. At  $r/a=0.3$  [Fig. 3(b)] the  $E \times B$  shear increased and the low  $k$  modes became more stable. Again only the high- $k$  ETG modes show an increase in growth rate. At larger radii [ $r/a=0.4$ , Fig. 3(c),  $r/a=0.5$ , Fig. 3(d)], both the growth rates and the  $E \times B$  shear rates drop. The low- $k$  growth rate exceeds the  $E \times B$  shearing rate at  $r/a=0.5$  after the fastwave heating. A greater drop in the  $E \times B$  shear than in the growth rate is characteristic of a bifurcation back to active ITG turbulence [4]. In summary, the destabilization of the ETG mode is consistent with the increased power balance electron thermal transport within the ITB ( $r/a \leq 0.3$ ) after the fastwave heating. The loss of  $E \times B$  shear suppression of ITG/TEM modes at  $r/a=0.5$  is consistent with the retreat of the leading edge of the ITB. In order to study the dynamics of this discharge a simple transport model has been used in the ONETWO code. The model has a turbulent diffusivity which depends upon the electron temperature gradient and which includes the  $E \times B$  shear quench rule. A constant multiplier is applied to the neoclassical diffusivities to increase the background transport level. The model given below was used in the calculations shown in Fig. 4.

$$\begin{aligned}
 \chi_s &= \chi^A + C_s \chi_s^{\text{NEO}}, \quad s = (i, e, n, v) \\
 \chi^A &= C^A \rho_i^2 (\gamma - |\omega_{E \times B}|) \text{ for } \gamma > |\omega_{E \times B}|, \quad = 0 \text{ for } \gamma < |\omega_{E \times B}| \\
 \gamma &= 0.1 (q v_{\text{th}} / R) \sqrt{|R / L_{Te}|}, \quad \rho_i = \text{ion gyroradius}, \quad v_{\text{th}} = \sqrt{T_e m_i} \\
 \omega_{E \times B} &= (R B_p / B_T) d(E_r / R B_p) / dr \\
 C_i &= 1, \quad C_e = 156, \quad C_n = 2, \quad C_v = 44
 \end{aligned} \tag{1}$$

All of the profiles were evolved to steady state [electron (e) and ion (i) temperatures, electron density (n), ion toroidal rotation (v) and poloidal magnetic field ( $B_p$ )]. The  $E \times B$  shear was computed self-consistently from the ion radial force balance using a neoclassical

calculation for the poloidal velocity contribution. The heating was 6 MW of co-injected NBI and 6 MW of ECH with the deposition profile shown in Fig. 4(c). For ECH heating centered at  $r/a=0.3$ , (case B) there is little evidence of an ITB from the electron [Fig. 4(a)] and ion pressure [Fig. 4(b)] profiles but in fact the ion thermal diffusivity [Fig. 4(d)] is neoclassical for  $r/a \leq 0.2$ . For ECH heating centered at  $r/a=0.7$  (case C) an ITB extends to  $r/a \leq 0.6$ . The explanation of this result is clear for the model. With just the neutral beams (case A) the co-toroidal rotation shear gave a weak ITB out to  $r/a=0.3$ . The ECH heating increases the electron heat flux at the heating location and at larger radii. This reduces the ratio of co-toroidal momentum injection to heating which reduces the  $E \times B$  shear [5] and causes the ITB to be difficult to extend past the ECH heating radius. At smaller radii than the ECH absorption layer, the electron temperature rises but the heat flux conducted through the electron channel actually drops. This is because higher electron temperature reduces the neutral beam electron heating, the Ohmic heating and the ion to electron heat exchange. Since the model for the anomalous transport is driven by the normalized electron temperature gradient ( $R/L_{Te}$ ), the reduced electron heating makes it easier for the ITB to exist at radii smaller than the absorption layer. Thus, for both heating locations, the ITB tends to exist only at smaller radii than the ECH absorption layer. This is how the model works but how does this relate to the experiment? The model is imperfect in many ways but the ETG mode transport could yield a similar effect. Even if the ETG mode only affects the electron thermal transport, as predicted by quasilinear theory, a change in electron heat transport can change the fraction of power conducted through the ion channel and hence the  $E \times B$  shear indirectly. If the ETG modes affect ion thermal or particle transport directly, then since the ETG modes are not stabilized by the  $E \times B$  shear levels achieved in the experiment, electron heating would have a similar effect on the ITB as found from the model.

## REFERENCES

- [1] M. Kotschenreuther *et al.*, Comput. Phys. Commun. **88**, 128 (1995).
- [2] K.H. Burrell, Phys. Plasmas **4**, 1499 (1997).
- [3] R.E. Waltz *et al.*, Phys. Plasmas **1**, 2229 (1994); Phys. Plasmas **5**, 1794 (1998).
- [4] G.M. Staebler *et al.*, Proc. 24th EPS Conf. on Contr. Fusion and Plasma Phys., Berchtesgaden, 9-13 June, 1997, P3-1097.
- [5] G. M. Staebler *et al.*, Nucl. Fusion **37**, 287 (1997).

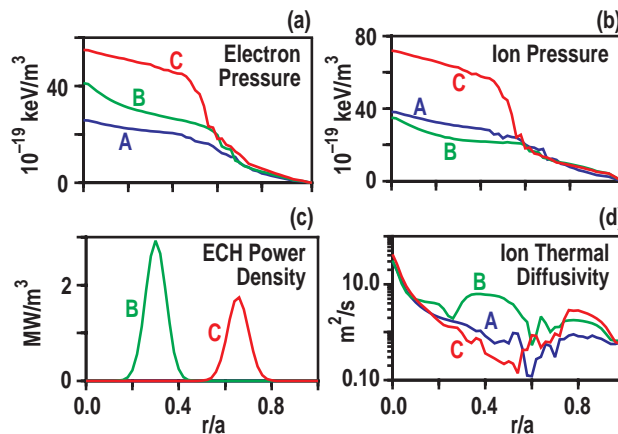


Fig. 4. Computed profiles of electron pressure (a) and ion pressure (b) using the transport model Eq. (1). Three cases are shown all with 6 MW of co-NBI (A) no ECH, (B) 6 MW ECH at  $r/a=0.3$ , (C) 6 MW ECH at  $r/a=0.7$  [see panel(c)]. Also shown is the ion thermal diffusivity from the model (d).